

Fermi sea term in the relativistic linear muffin-tin-orbital transport theory for random alloys

I. Turek*

Institute of Physics of Materials, Academy of Sciences of the Czech Republic, Žitkova 22, CZ-616 62 Brno, Czech Republic

J. Kudrnovský[†] and V. Drchal[‡]

*Institute of Physics, Academy of Sciences of the Czech Republic,
Na Slovance 2, CZ-182 21 Praha 8, Czech Republic*

(Dated: February 10, 2014)

We present a formulation of the so-called Fermi sea contribution to the conductivity tensor of spin-polarized random alloys within the fully relativistic tight-binding linear muffin-tin-orbital (TB-LMTO) method and the coherent potential approximation (CPA). We show that the configuration averaging of this contribution leads to the CPA-vertex corrections that are solely due to the energy dependence of the average single-particle propagators. Moreover, we prove that this contribution is indispensable for the invariance of the anomalous Hall conductivities with respect to the particular LMTO representation used in numerical implementation. *Ab initio* calculations for cubic ferromagnetic 3d transition metals (Fe, Co, Ni) and their random binary alloys (Ni-Fe, Fe-Si) indicate that the Fermi sea term is small against the dominating Fermi surface term. However, for more complicated structures and systems, such as hexagonal cobalt and selected ordered and disordered Co-based Heusler alloys, the Fermi sea term plays a significant role in the quantitative theory of the anomalous Hall effect.

PACS numbers: 72.10.Bg, 72.15.Gd, 75.47.Np

I. INTRODUCTION

The simultaneous presence of a spontaneous spin polarization and spin-orbit interaction in a solid gives rise to a number of physically interesting and technologically important phenomena, such as, e.g., magnetocrystalline anisotropy or magnetic dichroism in the X-ray absorption spectra.¹ The anomalous Hall effect^{2–4} (AHE) represents the most famous example of a spin-orbit driven transverse transport phenomenon in itinerant magnets; these phenomena include also the anomalous Nernst effect^{5,6} as a thermal analog of the AHE. The current understanding of the AHE rests on the identification of the basic underlying mechanisms,^{3,4,7} namely, the Berry curvature of occupied Bloch states for perfect crystals^{8,9} and the skew scattering^{10,11} and side-jump¹² mechanisms for systems with impurities. The present state of the theory of the AHE can be documented by ample model studies explaining the observed relation between the anomalous Hall conductivity (AHC) and the longitudinal conductivity in different regimes, ranging from low to high conductivities, see Ref. 4 and 6 and references therein.

Recently, first-principles studies of specific materials have appeared, devoted to pure ferromagnetic metals^{13–15} and various ordered compounds,^{16–18} including spin-gapless semiconductors¹⁹ and non-collinear antiferromagnets.²⁰ The latest trend in this field is featured by a development of techniques applicable to a wide class of systems, covering both clean crystals and diluted as well as concentrated random alloys, with the inclusion of all contributions to the AHE on equal footing. Existing studies are based on the single-particle Green's function (GF) and the coherent potential approximation (CPA) in the framework of the fully relativistic Korringa-Kohn-Rostoker (KKR)²¹ or the tight-binding linear muffin-tin-orbital (TB-LMTO)²² methods. Both approaches employ the conductivity tensor formulated in the Kubo linear response theory,²³ where the corresponding configuration averaging leads to the so-called CPA-vertex corrections.^{24–26}

Most of the published results for random alloys^{21,22,27–29} rest on the Kubo-Středa formula,^{7,30} which provides an expression for the full conductivity tensor at zero temperature solely in terms of quantities at the Fermi energy. However, the calculations could be performed only with the neglect of a term containing – in addition to the usual velocity operators – also the coordinate operator. This last operator is not compatible with periodic boundary conditions used in standard bulk techniques; the neglect of the problematic term has been justified by a high degree of symmetry of the crystal lattice (e.g., cubic).^{21,22} The neglected term is equivalent to the so-called Fermi sea contribution which follows from the original Bastin formula for the conductivity tensor.³¹ The Fermi sea term does not contain any coordinate operator, but it requires energy integration over the occupied part of the valence spectrum. Its direct evaluation for model systems³² and for realistic band structures of transition metals³³ indicates that, at least in the high-conductivity regime, the Fermi sea term represents a small correction to the dominating Fermi surface term defined only in terms of quantities at the Fermi energy. However, similar studies for the qualitatively different systems mentioned above cannot be found in the literature.

The present study is devoted to a formulation of the conductivity tensor from the Bastin formula in the relativistic TB-LMTO method; the focus is on the Fermi sea term and random alloys. Our approach employs several differences between the TB-LMTO and KKR methods. First, the transport in the TB-LMTO method is described as intersite hopping between neighboring atomic (Wigner-Seitz) cells, which leads to non-random (configuration independent) effective velocity operators,³⁴ while the KKR method rests on velocities represented by random site-diagonal matrices.²⁵ This feature is advantageous especially in the formulation of the vertex corrections in the TB-LMTO-CPA approach. Second, the LMTO structure constants are energy independent in contrast to the energy dependent KKR structure constants. Third, the scattering properties of individual atoms are described by simple analytic functions of energy in the LMTO method, whereas the full energy dependence of the single-site T-matrices in the KKR method is obtained by numerical integration of the radial Schrödinger or Dirac equation.^{35,36} The last two properties are used in the calculation of the energy derivative of the GF which enters the Fermi sea term.

The paper is organized as follows. The theoretical part is summarized in Section II, with Section II A devoted to the general form of the conductivity tensor and Section II B explaining the configuration averaging of the Fermi sea term. The technical aspects of the energy derivative of the coherent potential function, appearing in the final formula, are presented in Appendix A. The LMTO transformation properties of individual parts of the derived conductivity tensor are listed in Section II C while the corresponding details can be found in Appendix B. Information on the numerical implementation is given in Section II D. Illustrating examples of the calculated AHCs are summarized in Section III; the case of pure metals is contained in Section III A and that of random alloys and compounds is discussed in Section III B. The main conclusions are presented in Section IV.

II. METHOD

A. Conductivity tensor from the Bastin formula

Our starting point is the so-called Bastin formula for the conductivity tensor $\sigma_{\mu\nu}$ of a non-interacting electron system

$$\sigma_{\mu\nu} = -2\sigma_0 \int dE f(E) \text{Tr} \langle V_\mu G'_+(E) V_\nu [G_+(E) - G_-(E)] - V_\mu [G_+(E) - G_-(E)] V_\nu G'_-(E) \rangle, \quad (1)$$

which is well documented in the literature.^{7,30,31,37} The subscripts μ and ν in (1) are indices of Cartesian coordinates ($\mu, \nu \in \{x, y, z\}$), the integral is taken over the whole real energy axis, the function $f(E)$ denotes the Fermi-Dirac distribution function, the symbol V_μ denotes the velocity operator and the $G_\pm(E) = \lim_{\epsilon \rightarrow 0^+} G(E \pm i\epsilon)$ denote the side limits of the GF (resolvent) of the one-particle Hamiltonian H ,

$$G(z) = (z - H)^{-1}, \quad (2)$$

where z is a complex energy variable. The prime at the $G_\pm(E)$ denotes the energy derivative and the prefactor σ_0 is given by $\sigma_0 = e^2 \hbar / (4\pi V_0 N)$, where e denotes the electron charge, V_0 is the volume of the primitive cell, and N is the number of cells in a big finite crystal with periodic boundary conditions. The trace in (1) is taken over all orbitals of the Hilbert space of the crystal and the symbol $\langle \dots \rangle$ denotes the average over all configurations of the random alloy. The velocity operators (with $\hbar = 1$ assumed) are defined by a quantum-mechanical commutation relation as

$$V_\mu = -i[X_\mu, H], \quad (3)$$

where X_μ denotes the coordinate operator.

The Hamiltonian in the relativistic TB-LMTO method for spin-polarized systems can be written in the basis of orthonormal LMTO orbitals as^{22,38-40}

$$H = C + (\sqrt{\Delta})^+ [1 + S(\alpha - \gamma)]^{-1} S \sqrt{\Delta}, \quad (4)$$

where the symbols C , $\sqrt{\Delta}$ and γ denote site-diagonal matrices of the LMTO potential parameters while α denotes a site-diagonal matrix of the LMTO screening constants, which define both the corresponding LMTO representation and the matrix S of short-ranged (screened) structure constants.^{41,42} To simplify the formulas below, the index α of the particular LMTO representation is omitted in the main text of the paper including Appendix A, but it is restored in Appendix B.

The TB-LMTO method for disordered alloys^{39,40,43} employs the so-called auxiliary GF

$$g(z) = [P(z) - S]^{-1}, \quad (5)$$

where $P(z)$ denotes a site-diagonal matrix of potential functions. Note that the potential functions $P(z)$ as well as the potential parameters C , $\sqrt{\Delta}$ and γ are random quantities, depending on the occupation of the lattice sites \mathbf{R} by atomic species of the alloy, whereas the structure-constant matrix S and the matrix α of screening constants are non-random. The configuration average of the $g(z)$ in the single-site CPA is given by

$$\langle g(z) \rangle = \bar{g}(z) = [\mathcal{P}(z) - S]^{-1}, \quad (6)$$

where $\mathcal{P}(z)$ denotes a non-random site-diagonal matrix of the so-called coherent potential functions.

The TB-LMTO transport studies^{22,34} rest on a systematic disregarding of electron motion inside the atomic spheres, which leads to non-random effective velocities defined by

$$v_\mu = -i[X_\mu, S]. \quad (7)$$

The coordinate operators in (7) are represented by site- and orbital-diagonal matrices

$$(X_\mu)_{\mathbf{R}\mathbf{R}'}^{LL'} = \delta_{\mathbf{R}\mathbf{R}'} \delta^{LL'} X_{\mathbf{R}}^\mu, \quad (8)$$

where $X_{\mathbf{R}}^\mu$ is the μ th component of the position vector \mathbf{R} and L denotes the orbital index. Note that the index L in this paper labels all orbitals belonging to a single site; its detailed structure in the spin-polarized relativistic formalism has been given elsewhere.^{22,39,40}

It was shown in our previous study²² that the original velocity (3) is related to its effective counterpart (7) by a simple rescaling

$$V_\mu = (\sqrt{\Delta})^+ F^{-1} v_\mu (F^+)^{-1} \sqrt{\Delta}, \quad (9)$$

where the factor F is explicitly given by

$$F = 1 + S(\alpha - \gamma). \quad (10)$$

Similarly, the relation between the true resolvent (2) and the auxiliary GF (5) is given by a matrix shift and rescaling²²

$$G(z) = (\sqrt{\Delta})^{-1} F^+ [(\alpha - \gamma) + g(z)F] [(\sqrt{\Delta})^+]^{-1}. \quad (11)$$

Since the quantities α , γ , $\sqrt{\Delta}$ and F are energy independent, the last relation simplifies for energy derivatives of the GFs to

$$G'(z) = (\sqrt{\Delta})^{-1} F^+ g'(z) F [(\sqrt{\Delta})^+]^{-1}, \quad (12)$$

and for differences of the GFs to

$$G(z_1) - G(z_2) = (\sqrt{\Delta})^{-1} F^+ [g(z_1) - g(z_2)] F [(\sqrt{\Delta})^+]^{-1}, \quad (13)$$

where z , z_1 and z_2 are arbitrary complex energies outside the spectrum of the Hamiltonian H . The use of Eqs. (9, 12, 13) in the Bastin formula (1) leads immediately to the following expression for the conductivity tensor:

$$\begin{aligned} \sigma_{\mu\nu} = -2\sigma_0 \int dE f(E) \text{Tr} \langle & v_\mu g'_+(E) v_\nu [g_+(E) - g_-(E)] \\ & - v_\mu [g_+(E) - g_-(E)] v_\nu g'_-(E) \rangle. \end{aligned} \quad (14)$$

This form is identical with the original one, but the derived Eq. (14) has clear advantages in the configuration averaging for two reasons. First, the full resolvents $G_\pm(E)$ are replaced by the auxiliary GFs for which the CPA-average $\bar{g}(z)$ can be directly evaluated according to Eq. (6). Second, the random velocities V_μ are replaced by the non-random effective velocities v_μ so that the configuration average of the whole conductivity tensor can be performed by following the standard formulation of the CPA-vertex corrections.^{24,26}

Further processing of the expression (14) can be done along the well-known direction:⁷ one half of this expression is kept while the integration of the second half is performed by parts. The result is then rewritten as a sum of two terms,

$$\sigma_{\mu\nu} = \sigma_{\mu\nu}^{(1)} + \sigma_{\mu\nu}^{(2)}, \quad (15)$$

where the first term – the Fermi surface term – contains the integral with $f'(E)$, namely,

$$\sigma_{\mu\nu}^{(1)} = \sigma_0 \int dE f'(E) \text{Tr} \langle v_\mu g_+(E) v_\nu [g_+(E) - g_-(E)] - v_\mu [g_+(E) - g_-(E)] v_\nu g_-(E) \rangle, \quad (16)$$

while the second term – the Fermi sea term – contains the rest integral with $f(E)$, i.e.,

$$\sigma_{\mu\nu}^{(2)} = \sigma_0 \int dE f(E) \text{Tr} \langle v_\mu g_+(E) v_\nu g'_+(E) - v_\mu g'_+(E) v_\nu g_+(E) - v_\mu g_-(E) v_\nu g'_-(E) + v_\mu g'_-(E) v_\nu g_-(E) \rangle. \quad (17)$$

For systems with zero temperature, the Fermi surface term (16) can be written as

$$\sigma_{\mu\nu}^{(1)} = \sigma_0 \text{Tr} \langle v_\mu [g_+(E_F) - g_-(E_F)] v_\nu g_-(E_F) - v_\mu g_+(E_F) v_\nu [g_+(E_F) - g_-(E_F)] \rangle, \quad (18)$$

where E_F denotes the Fermi energy. The evaluation of this term within the relativistic LMTO approach has been described in Ref. 22 while the corresponding vertex corrections were formulated in detail in the Appendix of Ref. 26.

The zero-temperature case of the Fermi sea term (17) can be recast into a contour integral in the complex energy plane:

$$\sigma_{\mu\nu}^{(2)} = \sigma_0 \int_C dz \text{Tr} \langle v_\mu g'(z) v_\nu g(z) - v_\mu g(z) v_\nu g'(z) \rangle, \quad (19)$$

where the integration path C starts and ends at E_F , it is oriented counterclockwise and it encompasses the whole occupied part of the alloy valence spectrum. Note that the Fermi sea term is antisymmetric, $\sigma_{\mu\nu}^{(2)} = -\sigma_{\nu\mu}^{(2)}$, so that it contributes only to the AHCs while the longitudinal conductivities are given only by the Fermi surface term.

The derived expression (19) for the Fermi sea term, obtained from the Kubo-Bastin formulation of the conductivity tensor, can be transformed into the corresponding term of the Kubo-Středa formula, namely, $\sigma_{\mu\nu}^{(2)} = \sigma_0 \text{Tr} \langle i(X_\mu v_\nu - X_\nu v_\mu) [g_+(E_F) - g_-(E_F)] \rangle$, see the second term in Eq. (17) of Ref. 22. This transformation is formally exact,^{7,30} but the transformed result contains the coordinate operator that is unbounded and incompatible with the periodic boundary conditions used in the numerical implementation. For simple systems with inversion symmetry (cubic, hexagonal close-packed), the lattice summations can be rearranged in such a way that the resulting $\sigma_{\mu\nu}^{(2)}$ vanishes identically, in contrast to the results of Eq. (19), see Section III A. Since the Kubo-Bastin approach does not involve the problematic coordinate operator and since the direct evaluation of $\sigma_{\mu\nu}^{(2)}$ yields non-zero values even for the simplest systems,^{32,33} the derived formula (19) represents a correct version of the Fermi sea term within the TB-LMTO formalism.

B. Configuration averaging of the Fermi sea term

For the CPA-average of the Fermi sea term (19), we use the relation

$$\text{Tr} \langle v_\mu g'(z) v_\nu g(z) \rangle = \lim_{z_1 \rightarrow z} \frac{\partial}{\partial z_1} \text{Tr} \langle v_\mu g(z_1) v_\nu g(z) \rangle, \quad (20)$$

where the average on the r.h.s. can be split into the coherent part and the incoherent part (vertex corrections – VC):

$$\text{Tr} \langle v_\mu g(z_1) v_\nu g(z) \rangle = \text{Tr} \{ v_\mu \bar{g}(z_1) v_\nu \bar{g}(z) \} + \text{Tr} \langle v_\mu g(z_1) v_\nu g(z) \rangle_{\text{VC}}. \quad (21)$$

The second term can be written according to the general expression²⁶ as

$$\begin{aligned} \text{Tr} \langle v_\mu g(z_1) v_\nu g(z) \rangle_{\text{VC}} &= \sum_{\mathbf{R}_1 \Lambda_1} \sum_{\mathbf{R}_2 \Lambda_2} [\bar{g}(z) v_\mu \bar{g}(z_1)]_{\mathbf{R}_1 \mathbf{R}_1}^{L'_1 L_1} [\Delta^{-1}(z_1, z)]_{\mathbf{R}_1 \mathbf{R}_2}^{\Lambda_1 \Lambda_2} \\ &\quad \times [\bar{g}(z_1) v_\nu \bar{g}(z)]_{\mathbf{R}_2 \mathbf{R}_2}^{L_2 L'_2}, \end{aligned} \quad (22)$$

where the symbols Λ_1 and Λ_2 abbreviate the composed orbital indices $\Lambda_1 = (L_1, L'_1)$ and $\Lambda_2 = (L_2, L'_2)$ and where the matrix $\Delta_{\mathbf{R}_1 \mathbf{R}_2}^{\Lambda_1 \Lambda_2}(z_1, z_2)$ was defined in the Appendix of Ref. 26. The evaluation of the vertex contribution to Eq. (20) is greatly simplified due to the exact vanishing of the on-site blocks of the matrix product $\bar{g}(z) v_\mu \bar{g}(z)$:

$$[\bar{g}(z) v_\mu \bar{g}(z)]_{\mathbf{R} \mathbf{R}}^{LL'} = 0, \quad (23)$$

which is valid for the same energy arguments of both GFs. This rule is a consequence of the simple form of the coordinate operators X_μ (8) and of the single-site nature of the coherent potential functions $\mathcal{P}(z)$, i.e., $\mathcal{P}_{\mathbf{R}\mathbf{R}'}^{LL'}(z) = \delta_{\mathbf{R}\mathbf{R}'}\mathcal{P}_{\mathbf{R}}^{LL'}(z)$, from which we get $[\mathcal{P}(z), X_\mu] = 0$ and, by employing Eq. (6), also $\bar{g}(z)[X_\mu, S]\bar{g}(z) = \bar{g}(z)[\mathcal{P}(z) - S, X_\mu]\bar{g}(z) = [X_\mu, \bar{g}(z)]$. The validity of Eq. (23) follows now from the vanishing of the on-site blocks of the last commutator. After taking the partial derivative with respect to z_1 of Eq. (22), making the limit $z_1 \rightarrow z$, and using the rule (23), we get

$$\lim_{z_1 \rightarrow z} \frac{\partial}{\partial z_1} \text{Tr} \langle v_\mu g(z_1) v_\nu g(z) \rangle_{\text{VC}} = 0. \quad (24)$$

By employing this identity in Eqs. (20, 21), we obtain a simple result

$$\text{Tr} \langle v_\mu g'(z) v_\nu g(z) \rangle = \text{Tr} \{ v_\mu \bar{g}'(z) v_\nu \bar{g}(z) \}, \quad (25)$$

which can be used to rewrite the configurationally averaged Fermi sea term (19) as

$$\sigma_{\mu\nu}^{(2)} = \sigma_0 \int_C dz \text{Tr} \{ v_\mu \bar{g}'(z) v_\nu \bar{g}(z) - v_\mu \bar{g}(z) v_\nu \bar{g}'(z) \}. \quad (26)$$

This formula represents the main result of this Section.

The obtained result (26) could be interpreted as if the averaged Fermi sea contribution to the conductivity tensor contained only the coherent part. However, in the practical evaluation of the energy derivative $\bar{g}'(z)$, one has to use the relation

$$\bar{g}'(z) = -\bar{g}(z)\mathcal{P}'(z)\bar{g}(z), \quad (27)$$

which follows from the energy independent structure constants S in (6) and which leads to the final expression for the Fermi sea term:

$$\sigma_{\mu\nu}^{(2)} = \sigma_0 \int_C dz \text{Tr} \{ [v_\mu \bar{g}(z) v_\nu - v_\nu \bar{g}(z) v_\mu] \bar{g}(z) \mathcal{P}'(z) \bar{g}(z) \}. \quad (28)$$

As it is shown in Appendix A, the formulation of the energy derivative $\mathcal{P}'(z)$ leads to a set of linear equations that is very similar to that encountered in the formulation of the CPA-vertex corrections.²⁶ In other words, in the configuration average of the Fermi sea term, the vertex corrections corresponding to $\langle g(z) v_\mu g(z) \rangle$ vanish identically, but those appearing in $\bar{g}'(z) = -\langle g(z) \mathcal{P}'(z) g(z) \rangle$ do contribute. These last vertex corrections are related directly to the energy dependence of the averaged single-particle GF and to the Ward identity for the conservation of particle number;²⁴ their proper inclusion is thus inevitable for an internally consistent approximative theory of the conductivity tensor.

Let us discuss briefly properties of the Fermi sea term in the dilute limit of a random binary alloy $A_{1-c}B_c$, where $c \rightarrow 0^+$. The AHC exhibits a divergent behavior in this limit, that is due to the incoherent part (vertex corrections) of the Fermi surface term.²¹ The coherent potential function behaves for small concentrations c as⁴⁴

$$\mathcal{P}_{\mathbf{R}}(z) = P_{\mathbf{R}}^A(z) + ct_{\mathbf{R}}^B(z), \quad (29)$$

where it is assumed that the species-resolved potential functions $P_{\mathbf{R}}^A(z)$ and $P_{\mathbf{R}}^B(z)$ are concentration independent and where the $t_{\mathbf{R}}^B(z)$ denotes the single-site T-matrix of a single B impurity in the host A crystal, see Eq. (A1) with $\mathcal{P}_{\mathbf{R}}(z) = P_{\mathbf{R}}^A(z)$ and $P_{\mathbf{R}}(z) = P_{\mathbf{R}}^B(z)$. This regular concentration dependence of the $\mathcal{P}_{\mathbf{R}}(z)$ and the final form of $\sigma_{\mu\nu}^{(2)}$ (28) mean that the Fermi sea term behaves in general regularly in the dilute limit. The only exceptions to this rule might be due to a possible singularity of the impurity T-matrix $t_{\mathbf{R}}^B(z)$ at the Fermi energy. The limiting case of a clean A crystal ($c = 0$) is obtained by setting $\mathcal{P}_{\mathbf{R}}(z) = P_{\mathbf{R}}^A(z)$ in Eq. (28) as well as in all GFs; the total AHC is then finite and equivalent to that of the Berry-curvature approach.

C. Transformation properties of the conductivity tensor

The TB-LMTO method for perfect crystals can be formulated in a general LMTO representation specified by a set of site-diagonal screening constants.^{41,42} Most auxiliary quantities depend on the choice of the LMTO representation and they have to be transformed according to well-known relations when changing the LMTO representation, whereas all physical quantities remain invariant. These transformation properties have been successfully combined with the

CPA for one-particle quantities of random alloys, such as the average auxiliary GF $\bar{g}(z)$, the coherent potential function $\mathcal{P}(z)$, or the single-site T-matrices $t_{\mathbf{R}}(z)$.^{40,45} However, the case of two-particle quantities, in particular of the conductivity tensor, has not been treated so far. Here we summarize the most important results concerning the total tensor and its various contributions; the proof of our statements is outlined in Appendix B.

Let us write the conductivity tensor (15) as $\sigma_{\mu\nu} = \sigma_{\mu\nu,\text{coh}}^{(1)} + \sigma_{\mu\nu,\text{VC}}^{(1)} + \sigma_{\mu\nu}^{(2)}$, where the first and the second terms denote, respectively, the coherent and the incoherent (vertex) parts of the Fermi surface term (18). The following quantities are then invariant: (i) the total tensor $\sigma_{\mu\nu}$, (ii) the incoherent Fermi surface term $\sigma_{\mu\nu,\text{VC}}^{(1)}$, and (iii) the sum of the coherent Fermi surface term and of the Fermi sea term, $\sigma_{\mu\nu,\text{coh}}^{(1)} + \sigma_{\mu\nu}^{(2)}$. Since the Fermi sea term is antisymmetric, the last property means that the symmetric part of the coherent Fermi surface term, $[\sigma_{\mu\nu,\text{coh}}^{(1)} + \sigma_{\nu\mu,\text{coh}}^{(1)}]/2$, is invariant as well. These properties prove the importance of the Fermi sea term for the complete TB-LMTO-CPA theory of the AHE.

The above LMTO transformation properties together with the purely coherent nature of the Fermi sea term (26) and with its regular behavior in diluted alloys (end of Section II B) are relevant for a classification of the intrinsic and extrinsic contributions to the AHE.^{3,4,21} Within the present TB-LMTO formalism, the intrinsic AHC has to be identified with the antisymmetric part of the sum of the coherent Fermi surface term and of the Fermi sea term $[\sigma_{\mu\nu,\text{coh}}^{(1)} + \sigma_{\mu\nu}^{(2)}]$, whereas the extrinsic AHC is given by the antisymmetric part of the incoherent Fermi surface term $[\sigma_{\mu\nu,\text{VC}}^{(1)}]$. This seems to be a natural generalization of the classification introduced recently in the KKR method using the Kubo-Středa formula.^{21,27}

D. Implementation and numerical details

The numerical implementation of the developed scheme and the calculations discussed in Section III were done with similar parameters as described in our recent papers concerning both the fully relativistic selfconsistent electronic structures⁴⁶ and the Fermi surface term of the conductivity tensor.^{22,29} The particular LMTO representation used in the calculations is defined by the screening constants leading to the most localized real-space structure constants for the valence basis consisting of *s*-, *p*-, and *d*-type orbitals.^{41,42} For calculations of the Fermi surface term, a small imaginary part of $\pm 10^{-5}$ Ry has been added to the Fermi energy while in the evaluation of the Fermi sea term (28), the integration has been performed along a circular contour of a diameter 1.5 Ry.^{47,48} The contour integral was approximated by a sum over 20 – 40 complex nodes in the upper semicircle; the nodes were located in an asymmetric way which results in a denser mesh near the Fermi energy. The number of \mathbf{k} vectors sampling the Brillouin zone depends on the distance between the particular complex node and the Fermi energy; for the node closest to the Fermi energy, the total numbers of $\sim 10^8$ \mathbf{k} vectors have been used. Convergence tests with respect to the numbers of energy nodes and of \mathbf{k} vectors have been performed for each system, which guarantee the reliability of the results presented below. In the present study, we have included three shells of nearest neighbors in the screened structure-constant matrix of the body-centered cubic (bcc) lattice, in contrast to the two neighboring shells used in Refs. 22 and 29, which leads to slightly modified values of the Fermi surface terms. Moreover, in contrast to our previous studies, the sign convention of the AHC in the present study has been adopted according to other authors.^{13,17,21}

III. RESULTS AND DISCUSSION

A. Pure Fe, Co, and Ni

The calculated AHCs for pure Fe, Co and Ni, compared to the results of other authors and with measured low-temperature values,^{49–51} are shown in Table I. For the cubic metals, bcc Fe and face-centered cubic (fcc) Co and Ni, the magnetization direction was taken along the [001] direction while for hexagonal close-packed (hcp) Co, magnetization was considered pointing along the hexagonal *c* axis (easy axis) as well as lying in the *ab* plane perpendicular to it. Note that the theoretical approaches based on the Berry curvature^{13–15} include both the Fermi surface and the Fermi sea terms, whereas the published KKR results in Ref. 27 contain only the Fermi surface term.

The total AHCs calculated in this work are in reasonable agreement with other results obtained by using the local spin-density approximation (LSDA); in particular, the AHC of bcc Fe is in a fair agreement with the experiment, whereas bigger discrepancies are encountered for Co and, especially, for Ni. This last disagreement has been ascribed to electron correlations, not treated properly within the LSDA, the effect of which is particularly strong in Ni⁵² and partly also in Co.⁵³

TABLE I. The calculated and experimental values of the AHC (in S/cm) for ferromagnetic 3d transition metals. Two columns for hcp Co refer to the magnetization direction along the c axis (c) and in the ab plane (ab). The values of the Fermi sea term are displayed in parentheses.

	bcc Fe	hcp Co (c)	hcp Co (ab)	fcc Co	fcc Ni
This work	796 (179)	471 (181)	169 (66)	359 (−5)	−2432 (−17)
Berry curvature	751 ^a	481 ^b	116 ^b	249 ^b	−2203 ^c
KKR method	685 ^d	325 ^d		213 ^d	−2062 ^d
Experiment	1032 ^e	~ 813 ^b	~ 150 ^b	727 ^f	−1100 ^g

^a Reference 13.

^b Reference 15.

^c Reference 14.

^d Reference 27.

^e Reference 49.

^f Reference 50.

^g Reference 51.

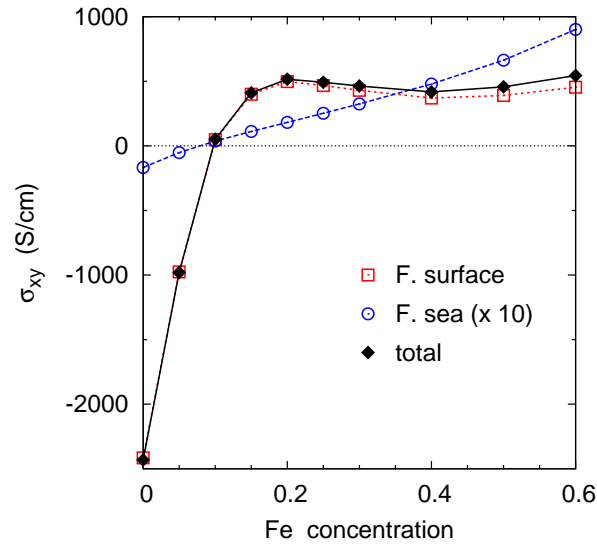


FIG. 1. (Color online) The calculated values of the total AHC (full diamonds) and its Fermi surface (open squares) and Fermi sea (open circles) contributions in random fcc $\text{Ni}_{1-c}\text{Fe}_c$ alloys as functions of Fe concentration. The values of the Fermi sea term are magnified by a factor of 10.

The calculated Fermi sea term is essentially negligible in fcc Co and Ni, and it represents a weak effect as compared to the Fermi surface term in bcc Fe. However, a completely different picture is obtained for hcp Co, where the Fermi sea term amounts nearly to 40% of the total AHC, irrespective of the orientation of the magnetization, i.e., the relative anisotropy of the Fermi sea term is similar to that of the Fermi surface term. The inclusion of the Fermi sea term brings the present TB-LMTO results in better agreement with those of the Berry-curvature approach and with the experiment.¹⁵ Our calculations prove that the previous statements^{21,22,33} about the dominating Fermi surface term in metallic systems with high longitudinal conductivities are not generally valid.

B. Random alloys and compounds

An example of the calculated AHC in a concentrated random alloy is presented in Fig. 1 for the fcc $\text{Ni}_{1-c}\text{Fe}_c$ system. One can see that the Fermi sea term represents a very small correction to the dominating Fermi surface term, as expected from the similar situation in the pure elements Fe and Ni. In particular, the previously discussed change of sign of the AHE, see Ref. 22 and references therein, is encountered at roughly the same concentration. Note that the Fermi sea term behaves in a smooth manner on the Ni-rich side despite the strong increase of the total AHC for $c \rightarrow 0$, in qualitative agreement with the conclusions drawn in Section II B.

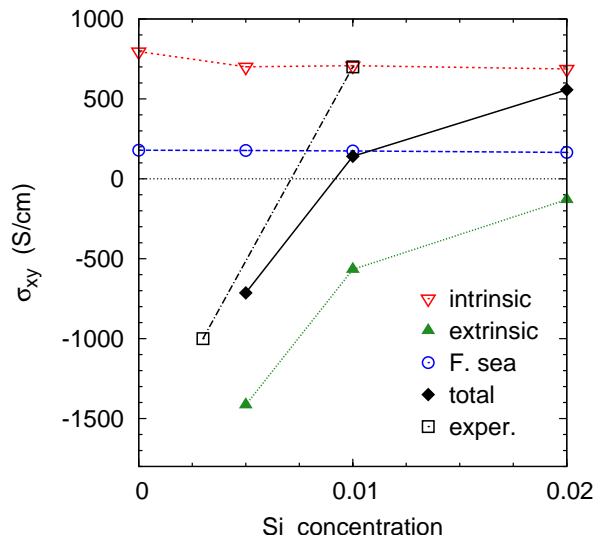


FIG. 2. (Color online) The calculated values of the total AHC (full diamonds) and its intrinsic (open triangles) and extrinsic (full triangles) parts in diluted bcc $\text{Fe}_{1-c}\text{Si}_c$ alloys as functions of Si concentration. The experimental AHC values⁵⁴ (open squares) and the calculated Fermi sea contributions (open circles) are displayed as well.

TABLE II. The calculated values of the AHC for selected ordered and disordered Co-based Heusler alloys. The values of the Fermi sea term are displayed in parentheses.

system	σ_{xy} (S/cm)
Ideal Co_2CrAl	400 (−107)
$(\text{Co}_{0.75}\text{Cr}_{0.25})_2(\text{Cr}_{0.5}\text{Co}_{0.5})\text{Al}$	144 (39)
$\text{Co}_2(\text{Cr}_{0.75}\text{Al}_{0.25})(\text{Al}_{0.75}\text{Cr}_{0.25})$	129 (4)
Ideal Co_2MnAl	1787 (728)
$\text{Co}_2(\text{Mn}_{0.75}\text{Al}_{0.25})(\text{Al}_{0.75}\text{Mn}_{0.25})$	452 (90)

Another case study concerns the high-conductivity regime of diluted bcc $\text{Fe}_{1-c}\text{Si}_c$ alloys, being motivated by recent experiments⁵⁴ for systems with Si impurity concentrations $c \leq 0.01$. The calculated AHCs are displayed in Fig. 2 together with the measured data; the total theoretical values were decomposed into the intrinsic and extrinsic parts as defined in Section II C. One can see a sign change of the AHC in a semiquantitative agreement with the experiment; this effect can be obviously ascribed to a strong variation of the extrinsic part, which diverges for $c \rightarrow 0$ due to the skew scattering mechanism, whereas the intrinsic part approaches smoothly the AHC of pure Fe. Note that the Fermi sea term, which enters the intrinsic part, is independent of the Si concentration and it becomes non-negligible for compositions with a very small total AHC. This system is an example of a ferromagnetic metal containing very light impurities with a negligible strength of the spin-orbit interaction and a weak exchange splitting. The diverging AHC and the change of its sign in the diluted Fe-Si alloy prove clearly that such light non-magnetic impurities in a ferromagnetic host with spin-orbit coupling can lead to pronounced skew-scattering effects in the transverse transport.⁴

The AHE has also been studied intensively in Co-based Heusler alloys Co_2CrAl and Co_2MnAl , both experimentally^{55,56} and theoretically.^{17,18,29} There is a generally accepted view that the structure and chemical composition of measured samples differ from those of ideal L_{21} compounds. These imperfections are responsible for a discrepancy between the calculated and measured magnetic moments, strong especially for the Co_2CrAl system, as well as for relatively high longitudinal resistivities of both systems. These facts have partly been explained by an antisite disorder,²⁹ assumed to be of the L_{21} type (Co-Cr swapping) or of the B2 type (Cr-Al swapping) in Co_2CrAl , and of the B2 type (Mn-Al swapping) in Co_2MnAl , in agreement with the experiment in the last case.⁵⁶ Detailed calculations of the electronic structure and of the AHE, based only on the Fermi surface term, were published in Ref. 29. Table II displays the total AHCs for both ideal compounds and for three disordered systems of compositions $(\text{Co}_{1-c}\text{Cr}_c)_2(\text{Cr}_{1-2c}\text{Co}_{2c})\text{Al}$ and $\text{Co}_2(\text{X}_{1-c}\text{Al}_c)(\text{Al}_{1-c}\text{X}_c)$ with $c = 0.25$ and $X = \text{Cr}, \text{Mn}$. The main conclusions of the previous study, namely, the strong reduction of the AHC of the ideal compounds by the antisite disorder and the small extrinsic (vertex corrections) part of the AHC,²⁹ are robust with respect to the inclusion of the Fermi sea term. The relative values

of the last term lie between 20 and 40 % of the total AHC; the only exception is the Co_2CrAl alloy with 25% of the Cr-Al swap, where the Fermi sea term is essentially negligible.

Let us mention also the inverse Heusler alloy Mn_2CoAl , which represents – in the ideal structure with a perfect stoichiometry and without antisite atoms – an example of the spin-gapless semiconductor.¹⁹ The AHE of this system at zero temperature is expected to vanish due to the absence of electron states at the Fermi energy. This property has been confirmed by recent theoretical calculations using the Berry-curvature approach¹⁹ and the Kubo-Středa formula.²⁹ The present calculation based on the Bastin formula leads to the Fermi surface and Fermi sea terms as well as to the total AHC smaller (in absolute values) than 0.5 S/cm, in very good agreement with the above theoretical expectation. Systematic calculations for the system with disorder and further analysis similar to that in Ref. 29 have to be left for future studies.

IV. CONCLUSIONS

We have extended our recent transport theory in the relativistic TB-LMTO method²² by a formulation and numerical implementation of the Fermi sea term, which follows from the Bastin formula for the conductivity tensor and which contributes to the AHE. In the case of random alloys treated in the CPA, the configuration averaging of this term revealed its purely coherent nature, with effective vertex corrections originating in the energy dependence of the average single-particle propagators. The behavior of the Fermi sea term in the dilute limit of a random alloy is in general regular, in contrast to the often diverging Fermi surface term. We have further examined the transformation properties of the conductivity tensor with respect to the choice of the LMTO representation. This analysis proved the importance of the Fermi sea term for the representation invariance of the total AHCs and of their intrinsic part.

The calculations performed with the best-screened LMTO representation for several qualitatively different systems confirmed in most cases an expected fact, namely, significantly smaller values of the Fermi sea term as compared to the Fermi surface term. Notable exceptions refer to uniaxial systems (hexagonal cobalt) and to multisublattice multicomponent systems (Heusler alloys). However, even in these cases, the inclusion of the Fermi sea term did not change qualitatively the most important features of the AHE, such as its anisotropy or sensitivity to antisite defects. It can be anticipated that the present theory will be useful in future first-principles studies of transverse transport properties of prospective materials, in particular with substitutional disorder.

ACKNOWLEDGMENTS

The authors acknowledge financial support by the Czech Science Foundation (Grant No. P204/11/1228).

Appendix A: Energy derivative of the coherent potential function

In this Appendix, the formulation of the energy derivative $\mathcal{P}'(z)$ is briefly sketched, which is based on the CPA-selfconsistency condition for the coherent potential function $\mathcal{P}(z)$. For brevity, the energy argument z of all quantities is omitted here.

In the single-site CPA, the coherent potential function is written as a lattice sum over individual sites, $\mathcal{P} = \sum_{\mathbf{R}} \mathcal{P}_{\mathbf{R}}$, and the single-site contributions $\mathcal{P}_{\mathbf{R}}$ are obtained from the vanishing of the average single-site T-matrix $t_{\mathbf{R}}$,

$$\langle t_{\mathbf{R}} \rangle = 0, \quad t_{\mathbf{R}} = [1 + (P_{\mathbf{R}} - \mathcal{P}_{\mathbf{R}})\bar{g}]^{-1} (P_{\mathbf{R}} - \mathcal{P}_{\mathbf{R}}). \quad (\text{A1})$$

The single-site contributions $\mathcal{P}'_{\mathbf{R}}$ to the energy derivative $\mathcal{P}' = \sum_{\mathbf{R}} \mathcal{P}'_{\mathbf{R}}$ can be obtained from the energy derivative of this selfconsistency condition. This yields:

$$\begin{aligned} \langle t'_{\mathbf{R}} \rangle &= 0, \\ t'_{\mathbf{R}} &= [1 + (P_{\mathbf{R}} - \mathcal{P}_{\mathbf{R}})\bar{g}]^{-1} (P'_{\mathbf{R}} - \mathcal{P}'_{\mathbf{R}}) \\ &\quad + [1 + (P_{\mathbf{R}} - \mathcal{P}_{\mathbf{R}})\bar{g}]^{-1} [-(P_{\mathbf{R}} - \mathcal{P}_{\mathbf{R}})\bar{g}' - (P'_{\mathbf{R}} - \mathcal{P}'_{\mathbf{R}})\bar{g}] t_{\mathbf{R}} \\ &= t_{\mathbf{R}}\bar{g}\mathcal{P}'\bar{g}t_{\mathbf{R}} + [1 + (P_{\mathbf{R}} - \mathcal{P}_{\mathbf{R}})\bar{g}]^{-1} (P'_{\mathbf{R}} - \mathcal{P}'_{\mathbf{R}})(1 - \bar{g}t_{\mathbf{R}}) \\ &= t_{\mathbf{R}}\bar{g}\mathcal{P}'\bar{g}t_{\mathbf{R}} + (1 - t_{\mathbf{R}}\bar{g})(P'_{\mathbf{R}} - \mathcal{P}'_{\mathbf{R}})(1 - \bar{g}t_{\mathbf{R}}), \end{aligned} \quad (\text{A2})$$

where we used the rule (27) and the identity $[1 + (P_{\mathbf{R}} - \mathcal{P}_{\mathbf{R}})\bar{g}]^{-1} = 1 - t_{\mathbf{R}}\bar{g}$, which follows from (A1). In the first

term on the r.h.s., we write explicitly $\mathcal{P}' = \sum_{\mathbf{R}'} \mathcal{P}'_{\mathbf{R}'}$, which leads to the form

$$0 = \sum_{\mathbf{R}'} \langle t_{\mathbf{R}} \bar{g} \mathcal{P}'_{\mathbf{R}'} \bar{g} t_{\mathbf{R}} \rangle + \langle (1 - t_{\mathbf{R}} \bar{g}) (P'_{\mathbf{R}} - \mathcal{P}'_{\mathbf{R}}) (1 - \bar{g} t_{\mathbf{R}}) \rangle. \quad (\text{A3})$$

In the lattice sum, we take out the contribution of the site $\mathbf{R}' = \mathbf{R}$. After a minor rearrangement of the terms and the use of the selfconsistency on the \mathbf{R} th site (A1), we get the final form of the condition for $\mathcal{P}'_{\mathbf{R}}$:

$$\mathcal{P}'_{\mathbf{R}} = \langle (1 - t_{\mathbf{R}} \bar{g}) P'_{\mathbf{R}} (1 - \bar{g} t_{\mathbf{R}}) \rangle + \sum_{\mathbf{R}' (\neq \mathbf{R})} \langle t_{\mathbf{R}} \bar{g} \mathcal{P}'_{\mathbf{R}'} \bar{g} t_{\mathbf{R}} \rangle. \quad (\text{A4})$$

This relation represents a set of coupled linear equations for the single-site contributions $\mathcal{P}'_{\mathbf{R}}$, which is very similar to that for single-site contributions $\Gamma_{\mathbf{R}}$ to the quantity $\Gamma = \sum_{\mathbf{R}} \Gamma_{\mathbf{R}}$ relevant for the general LMTO CPA-vertex corrections.²⁶ Note that the only difference between Eq. (A5) of Ref. 26 and the present Eq. (A4) is in the first term on the r.h.s. The solution for the $\mathcal{P}'_{\mathbf{R}}$ can thus be obtained by a slightly modified approach described in detail in the Appendix of Ref. 26. The energy derivative $P'_{\mathbf{R}}$ of the random potential functions in the first term on the r.h.s. of (A4) is calculated analytically from the parametrized form of the potential functions $P_{\mathbf{R}}$. The final expression can be written as $P'_{\mathbf{R}} = \tilde{\mu}_{\mathbf{R}} \mu_{\mathbf{R}}$, where the single-site contributions to the random quantities $\mu = \sum_{\mathbf{R}} \mu_{\mathbf{R}}$ and $\tilde{\mu} = \sum_{\mathbf{R}} \tilde{\mu}_{\mathbf{R}}$ are given by Eq. (7) of Ref. 22.

Appendix B: Transformation invariance of the conductivity tensor

The study of the invariance of various quantities with respect to the choice of the LMTO representation is based on relations for the coherent potential functions and the structure constants in two different representations, denoted by superscripts α and β :

$$\mathcal{P}^{\alpha}(z) = [1 + \mathcal{P}^{\beta}(z)(\beta - \alpha)]^{-1} \mathcal{P}^{\beta}(z), \quad S^{\alpha} = [1 + S^{\beta}(\beta - \alpha)]^{-1} S^{\beta}, \quad (\text{B1})$$

where the quantities α and β in the brackets denote non-random site-diagonal matrices of the screening constants.^{40,42} Let us abbreviate

$$K = 1 + S^{\beta}(\beta - \alpha), \quad K^{+} = 1 + (\beta - \alpha)S^{\beta}, \quad (\text{B2})$$

and $\bar{g}_{\pm} = \lim_{\epsilon \rightarrow 0+} \bar{g}(E_{\text{F}} \pm i\epsilon)$ [and similarly for other energy dependent quantities, such as the coherent potential functions $\mathcal{P}(z)$ and the single-site T-matrices $t_{\mathbf{R}}(z)$]. The transformation properties of the effective velocities (7) and of the average auxiliary GFs (6) and their energy derivatives can be summarized as

$$\begin{aligned} v_{\mu}^{\alpha} &= K^{-1} v_{\mu}^{\beta} (K^{+})^{-1}, & \bar{g}^{\alpha}(z) &= K^{+} \bar{g}^{\beta}(z) K + K^{+}(\beta - \alpha), \\ \bar{g}_{+}^{\alpha} - \bar{g}_{-}^{\alpha} &= K^{+}(\bar{g}_{+}^{\beta} - \bar{g}_{-}^{\beta}) K, & \bar{g}'^{\alpha}(z) &= K^{+} \bar{g}'^{\beta}(z) K, \end{aligned} \quad (\text{B3})$$

which can be proved by procedures similar to those found in Ref. 22 and 42.

The transformation of the coherent part of the Fermi surface term (18) is

$$\sigma_{\mu\nu, \text{coh}}^{(1), \alpha} = \sigma_0 \text{Tr} \{ v_{\mu}^{\alpha} (\bar{g}_{+}^{\alpha} - \bar{g}_{-}^{\alpha}) v_{\nu}^{\alpha} \bar{g}_{-}^{\alpha} - v_{\mu}^{\alpha} \bar{g}_{+}^{\alpha} v_{\nu}^{\alpha} (\bar{g}_{+}^{\alpha} - \bar{g}_{-}^{\alpha}) \} = \sigma_{\mu\nu, \text{coh}}^{(1), \beta} + Z_{\mu\nu}, \quad (\text{B4})$$

where the remainder is

$$Z_{\mu\nu} = \sigma_0 \text{Tr} \left\{ v_{\mu}^{\beta} (\bar{g}_{+}^{\beta} - \bar{g}_{-}^{\beta}) v_{\nu}^{\beta} (\beta - \alpha) K^{-1} - v_{\mu}^{\beta} (\beta - \alpha) K^{-1} v_{\nu}^{\beta} (\bar{g}_{+}^{\beta} - \bar{g}_{-}^{\beta}) \right\}. \quad (\text{B5})$$

This can be rewritten as

$$\begin{aligned} Z_{\mu\nu} &= \sigma_0 \text{Tr} \left\{ Y_{\mu\nu} (\bar{g}_{+}^{\beta} - \bar{g}_{-}^{\beta}) \right\}, \\ Y_{\mu\nu} &= v_{\mu}^{\beta} (\alpha - \beta) K^{-1} v_{\nu}^{\beta} - v_{\nu}^{\beta} (\alpha - \beta) K^{-1} v_{\mu}^{\beta}, \end{aligned} \quad (\text{B6})$$

which proves that for metallic systems, the coherent part of $\sigma_{\mu\nu}^{(1)}$ depends on the particular LMTO representation. Note, however, that $Y_{\mu\nu} = -Y_{\nu\mu}$ and $Z_{\mu\nu} = -Z_{\nu\mu}$, so that this dependence concerns only the antisymmetric part of the $\sigma_{\mu\nu, \text{coh}}^{(1)}$ tensor (related to the AHC). The symmetric part of $\sigma_{\mu\nu, \text{coh}}^{(1)}$ (related to longitudinal conductivities) is thus invariant with respect to the choice of the LMTO representation.

The Fermi sea term (26) transforms as

$$\sigma_{\mu\nu}^{(2),\alpha} = \sigma_0 \int_C dz \text{Tr} \{ v_\mu^\alpha \bar{g}'^\alpha(z) v_\nu^\alpha \bar{g}^\alpha(z) - v_\mu^\alpha \bar{g}^\alpha(z) v_\nu^\alpha \bar{g}'^\alpha(z) \} = \sigma_{\mu\nu}^{(2),\beta} + R_{\mu\nu}, \quad (\text{B7})$$

where the remainder is

$$R_{\mu\nu} = \sigma_0 \int_C dz \text{Tr} \{ v_\mu^\beta \bar{g}'^{\beta}(z) v_\nu^\beta (\beta - \alpha) K^{-1} - v_\mu^\beta (\beta - \alpha) K^{-1} v_\nu^\beta \bar{g}'^{\beta}(z) \}. \quad (\text{B8})$$

This remainder can be rewritten with the use of $\int_C dz \bar{g}'^\beta(z) = \bar{g}_-^\beta - \bar{g}_+^\beta$. After a minor rearrangement, we get

$$R_{\mu\nu} = -\sigma_0 \text{Tr} \{ Y_{\mu\nu} (\bar{g}_+^\beta - \bar{g}_-^\beta) \}, \quad (\text{B9})$$

which yields $R_{\mu\nu} + Z_{\mu\nu} = 0$. This proves that the Fermi sea term alone is sensitive to the choice of the LMTO representation, but the sum $\sigma_{\mu\nu, \text{coh}}^{(1)} + \sigma_{\mu\nu}^{(2)}$ is strictly invariant, as mentioned in Section II C.

For the vertex part of the Fermi surface term, transformation properties are needed for a number of quantities entering the general expression for the LMTO vertex corrections,²⁶ see also Eq. (22). For the average auxiliary GFs, it holds

$$\bar{g}^\alpha(z) = K^+ \bar{g}^\beta(z) \mathcal{P}^\beta(z) \mathcal{P}^{-\alpha}(z) = \mathcal{P}^{-\alpha}(z) \mathcal{P}^\beta(z) \bar{g}^\beta(z) K, \quad (\text{B10})$$

where we abbreviated $\mathcal{P}^{-\alpha}(z) = [\mathcal{P}^\alpha(z)]^{-1}$. The quantity $\tilde{g}(z)$ comprising all non-site-diagonal blocks of $\bar{g}(z)$, i.e., $\tilde{g}_{\mathbf{R}_1 \mathbf{R}_2}^{L_1 L_2}(z) = (1 - \delta_{\mathbf{R}_1 \mathbf{R}_2}) \bar{g}_{\mathbf{R}_1 \mathbf{R}_2}^{L_1 L_2}(z)$, transforms as

$$\tilde{g}^\alpha(z) = \mathcal{P}^{-\alpha}(z) \mathcal{P}^\beta(z) \tilde{g}^\beta(z) \mathcal{P}^\beta(z) \mathcal{P}^{-\alpha}(z). \quad (\text{B11})$$

The transformation rule for the quantity $\chi_{\mathbf{R}_1 \mathbf{R}_2}^{\Lambda_1 \Lambda_2} = (\tilde{g}_+)^{L_1 L_2}_{\mathbf{R}_1 \mathbf{R}_2} (\tilde{g}_-)^{L'_2 L'_1}_{\mathbf{R}_2 \mathbf{R}_1}$, where $\Lambda_1 = (L_1, L'_1)$, $\Lambda_2 = (L_2, L'_2)$, follows directly from Eq. (B11). One obtains

$$\chi^\alpha = \Pi \chi^\beta \tilde{\Pi}, \quad (\text{B12})$$

where we introduced site-diagonal quantities $\Pi_{\mathbf{R}_1 \mathbf{R}_2}^{\Lambda_1 \Lambda_2} = \delta_{\mathbf{R}_1 \mathbf{R}_2} \Pi_{\mathbf{R}_1}^{\Lambda_1 \Lambda_2}$ and $\tilde{\Pi}_{\mathbf{R}_1 \mathbf{R}_2}^{\Lambda_1 \Lambda_2} = \delta_{\mathbf{R}_1 \mathbf{R}_2} \tilde{\Pi}_{\mathbf{R}_1}^{\Lambda_1 \Lambda_2}$, where

$$\begin{aligned} \Pi_{\mathbf{R}}^{\Lambda_1 \Lambda_2} &= \left(\mathcal{P}_{+, \mathbf{R}}^{-\alpha} \mathcal{P}_{+, \mathbf{R}}^\beta \right)^{L_1 L_2} \left(\mathcal{P}_{-, \mathbf{R}}^\beta \mathcal{P}_{-, \mathbf{R}}^{-\alpha} \right)^{L'_2 L'_1}, \\ \tilde{\Pi}_{\mathbf{R}}^{\Lambda_1 \Lambda_2} &= \left(\mathcal{P}_{+, \mathbf{R}}^\beta \mathcal{P}_{+, \mathbf{R}}^{-\alpha} \right)^{L_1 L_2} \left(\mathcal{P}_{-, \mathbf{R}}^{-\alpha} \mathcal{P}_{-, \mathbf{R}}^\beta \right)^{L'_2 L'_1}. \end{aligned} \quad (\text{B13})$$

The single-site T-matrices (A1) transform according to^{40,45}

$$t_{\mathbf{R}}^\beta(z) = \mathcal{P}_{\mathbf{R}}^\beta(z) \mathcal{P}_{\mathbf{R}}^{-\alpha}(z) t_{\mathbf{R}}^\alpha(z) \mathcal{P}_{\mathbf{R}}^{-\alpha}(z) \mathcal{P}_{\mathbf{R}}^\beta(z), \quad (\text{B14})$$

and the site-diagonal quantity $w_{\mathbf{R}_1 \mathbf{R}_2}^{\Lambda_1 \Lambda_2} = \delta_{\mathbf{R}_1 \mathbf{R}_2} w_{\mathbf{R}_1}^{\Lambda_1 \Lambda_2}$, where $w_{\mathbf{R}}^{\Lambda_1 \Lambda_2} = \langle t_{+, \mathbf{R}}^{L_1 L_2} t_{-, \mathbf{R}}^{L'_2 L'_1} \rangle$, satisfies the transformation relation

$$w^\beta = \tilde{\Pi} w^\alpha \Pi. \quad (\text{B15})$$

As a consequence of the rules (B12) and (B15), the matrix $\Delta = w^{-1} - \chi$ and its inverse transform as

$$\Delta^\alpha = \Pi \Delta^\beta \tilde{\Pi}, \quad (\Delta^\alpha)^{-1} = \tilde{\Pi}^{-1} (\Delta^\beta)^{-1} \Pi^{-1}. \quad (\text{B16})$$

For transformations of the on-site blocks $(\bar{g}_+ v_\mu \bar{g}_-)^{L_1 L'_1}_{\mathbf{R} \mathbf{R}} \equiv (\bar{g}_+ v_\mu \bar{g}_-)^{\Lambda_1}_{\mathbf{R}}$ and $(\bar{g}_- v_\mu \bar{g}_+)^{L'_2 L_2}_{\mathbf{R} \mathbf{R}} \equiv (\bar{g}_- v_\mu \bar{g}_+)^{\tilde{\Lambda}_1}_{\mathbf{R}}$, one can use the previous relations (B3) and (B10) for v_μ and \bar{g}_\pm , respectively. The result is

$$(\bar{g}_+ v_\mu \bar{g}_-)^{\Lambda_1}_{\mathbf{R}} = \sum_{\Lambda_2} \Pi_{\mathbf{R}}^{\Lambda_1 \Lambda_2} (\bar{g}_+ v_\mu \bar{g}_-)^{\Lambda_2}_{\mathbf{R}}, \quad (\bar{g}_- v_\mu \bar{g}_+)^{\tilde{\Lambda}_1}_{\mathbf{R}} = \sum_{\Lambda_2} (\bar{g}_- v_\mu \bar{g}_+)^{\Lambda_2}_{\mathbf{R}} \tilde{\Pi}_{\mathbf{R}}^{\Lambda_2 \tilde{\Lambda}_1}, \quad (\text{B17})$$

where the $\tilde{\Lambda}_1 = (L'_1, L_1)$ and $\tilde{\Lambda}_2 = (L'_2, L_2)$ denote indices transposed to $\Lambda_1 = (L_1, L'_1)$ and $\Lambda_2 = (L_2, L'_2)$, respectively.

The calculation of the vertex part of the Fermi surface term (18) rests on the formula (22). The identity (23) yields $\text{Tr} \langle v_\mu g_+ v_\nu g_+ \rangle_{\text{VC}} = \text{Tr} \langle v_\mu g_- v_\nu g_- \rangle_{\text{VC}} = 0$, so that $\sigma_{\mu\nu, \text{VC}}^{(1)} = 2\sigma_0 \text{Tr} \langle v_\mu g_+ v_\nu g_- \rangle_{\text{VC}}$ and

$$\sigma_{\mu\nu, \text{VC}}^{(1), \alpha} = 2\sigma_0 \sum_{\mathbf{R}_1 \Lambda_1} \sum_{\mathbf{R}_2 \Lambda_2} (\bar{g}_-^\alpha v_\mu^\alpha \bar{g}_+^\alpha)_{\mathbf{R}_1}^{\tilde{\Lambda}_1} [(\Delta^\alpha)^{-1}]_{\mathbf{R}_1 \mathbf{R}_2}^{\Lambda_1 \Lambda_2} (\bar{g}_+^\alpha v_\nu^\alpha \bar{g}_-^\alpha)_{\mathbf{R}_2}^{\Lambda_2}. \quad (\text{B18})$$

The last relation combined with the transformations (B16) and (B17) leads to the invariance of the vertex corrections to the Fermi surface term, $\sigma_{\mu\nu, \text{VC}}^{(1), \alpha} = \sigma_{\mu\nu, \text{VC}}^{(1), \beta}$. This completes the proof of the invariance of the total conductivity tensor $\sigma_{\mu\nu}$ (15).

* turek@ipm.cz

† kudrnov@fzu.cz

‡ drchal@fzu.cz

¹ P. Strange, *Relativistic Quantum Mechanics* (Cambridge University Press, 1998).

² E. Hall, *Philos. Mag.* **12**, 157 (1881).

³ N. A. Sinitsyn, *J. Phys.: Condens. Matter* **20**, 023201 (2008).

⁴ N. Nagaosa, J. Sinova, S. Onoda, A. H. MacDonald, and N. P. Ong, *Rev. Mod. Phys.* **82**, 1539 (2010).

⁵ D. Xiao, Y. Yao, Z. Fang, and Q. Niu, *Phys. Rev. Lett.* **97**, 026603 (2006).

⁶ S. Onoda, N. Sugimoto, and N. Nagaosa, *Phys. Rev. B* **77**, 165103 (2008).

⁷ A. Crépieux and P. Bruno, *Phys. Rev. B* **64**, 014416 (2001).

⁸ R. Karplus and J. M. Luttinger, *Phys. Rev.* **95**, 1154 (1954).

⁹ T. Jungwirth, Q. Niu, and A. H. MacDonald, *Phys. Rev. Lett.* **88**, 207208 (2002).

¹⁰ J. Smit, *Physica* **21**, 877 (1955).

¹¹ J. Smit, *Physica* **24**, 39 (1958).

¹² L. Berger, *Phys. Rev. B* **2**, 4559 (1970).

¹³ Y. Yao, L. Kleinman, A. H. MacDonald, J. Sinova, T. Jungwirth, D. S. Wang, E. Wang, and Q. Niu, *Phys. Rev. Lett.* **92**, 037204 (2004).

¹⁴ X. Wang, D. Vanderbilt, J. R. Yates, and I. Souza, *Phys. Rev. B* **76**, 195109 (2007).

¹⁵ E. Roman, Y. Mokrousov, and I. Souza, *Phys. Rev. Lett.* **103**, 097203 (2009).

¹⁶ I. V. Solov'yev, *Phys. Rev. B* **67**, 174406 (2003).

¹⁷ J. Kübler and C. Felser, *Phys. Rev. B* **85**, 012405 (2012).

¹⁸ J. C. Tung and G. Y. Guo, *New J. Phys.* **15**, 033014 (2013).

¹⁹ S. Ouardi, G. H. Fecher, C. Felser, and J. Kübler, *Phys. Rev. Lett.* **110**, 100401 (2013).

²⁰ H. Chen, Q. Niu, and A. H. MacDonald, *Phys. Rev. Lett.* **112**, 017205 (2014).

²¹ S. Lowitzer, D. Ködderitzsch, and H. Ebert, *Phys. Rev. Lett.* **105**, 266604 (2010).

²² I. Turek, J. Kudrnovský, and V. Drchal, *Phys. Rev. B* **86**, 014405 (2012).

²³ R. Kubo, *J. Phys. Soc. Jpn.* **12**, 570 (1957).

²⁴ B. Velický, *Phys. Rev.* **184**, 614 (1969).

²⁵ W. H. Butler, *Phys. Rev. B* **31**, 3260 (1985).

²⁶ K. Carva, I. Turek, J. Kudrnovský, and O. Bengone, *Phys. Rev. B* **73**, 144421 (2006).

²⁷ D. Ködderitzsch, K. Chadova, J. Minár, and H. Ebert, *New J. Phys.* **15**, 053009 (2013).

²⁸ J. Kudrnovský, V. Drchal, S. Khmelevskiy, and I. Turek, *Phys. Rev. B* **84**, 214436 (2011).

²⁹ J. Kudrnovský, V. Drchal, and I. Turek, *Phys. Rev. B* **88**, 014422 (2013).

³⁰ P. Středa, *J. Phys. C: Solid State Phys.* **15**, L717 (1982).

³¹ A. Bastin, C. Lewiner, O. Betbeder-Matibet, and P. Nozieres, *J. Phys. Chem. Solids* **32**, 1811 (1971).

³² H. Kontani, T. Tanaka, and K. Yamada, *Phys. Rev. B* **75**, 184416 (2007).

³³ T. Naito, D. S. Hirashima, and H. Kontani, *Phys. Rev. B* **81**, 195111 (2010).

³⁴ I. Turek, J. Kudrnovský, V. Drchal, L. Szunyogh, and P. Weinberger, *Phys. Rev. B* **65**, 125101 (2002).

³⁵ J. Zablouil, R. Hammerling, L. Szunyogh, and P. Weinberger, *Electron Scattering in Solid Matter* (Springer, Berlin, 2005).

³⁶ H. Ebert, D. Ködderitzsch, and J. Minár, *Rep. Prog. Phys.* **74**, 096501 (2011).

³⁷ L. Smrčka and P. Středa, *J. Phys. C: Solid State Phys.* **10**, 2153 (1977).

³⁸ I. V. Solov'yev, A. I. Liechtenstein, V. A. Gubanov, V. P. Antropov, and O. K. Andersen, *Phys. Rev. B* **43**, 14414 (1991).

³⁹ A. B. Shick, V. Drchal, J. Kudrnovský, and P. Weinberger, *Phys. Rev. B* **54**, 1610 (1996).

⁴⁰ I. Turek, V. Drchal, J. Kudrnovský, M. Šob, and P. Weinberger, *Electronic Structure of Disordered Alloys, Surfaces and Interfaces* (Kluwer, Boston, 1997).

⁴¹ O. K. Andersen and O. Jepsen, *Phys. Rev. Lett.* **53**, 2571 (1984).

⁴² O. K. Andersen, Z. Pawłowska, and O. Jepsen, *Phys. Rev. B* **34**, 5253 (1986).

⁴³ J. Kudrnovský and V. Drchal, *Phys. Rev. B* **41**, 7515 (1990).

⁴⁴ B. Velický, S. Kirkpatrick, and H. Ehrenreich, *Phys. Rev.* **175**, 747 (1968).

- ⁴⁵ I. Turek, J. Kudrnovský, and V. Drchal, in *Electronic Structure and Physical Properties of Solids*, Lecture Notes in Physics, Vol. 535, edited by H. Dreyssé (Springer, Berlin, 2000) p. 349.
- ⁴⁶ I. Turek, J. Kudrnovský, and K. Carva, Phys. Rev. B **86**, 174430 (2012).
- ⁴⁷ A. R. Williams, P. J. Feibelman, and N. D. Lang, Phys. Rev. B **26**, 5433 (1982).
- ⁴⁸ R. Zeller, J. Deutz, and P. H. Dederichs, Solid State Commun. **44**, 993 (1982).
- ⁴⁹ P. N. Dheer, Phys. Rev. **156**, 637 (1967).
- ⁵⁰ D. Hou, Y. Li, D. Wei, D. Tian, L. Wu, and X. Jin, J. Phys.: Condens. Matter **24**, 482001 (2012).
- ⁵¹ L. Ye, Y. Tian, X. Jin, and D. Xiao, Phys. Rev. B **85**, 220403 (2012).
- ⁵² H. R. Fuh and G. Y. Guo, Phys. Rev. B **84**, 144427 (2011).
- ⁵³ J. C. Tung, H. R. Fuh, and G. Y. Guo, Phys. Rev. B **86**, 024435 (2012).
- ⁵⁴ Y. Shiomi, Y. Onose, and Y. Tokura, Phys. Rev. B **79**, 100404 (2009).
- ⁵⁵ A. Husmann and L. J. Singh, Phys. Rev. B **73**, 172417 (2006).
- ⁵⁶ E. V. Vidal, G. Stryganyuk, H. Schneider, C. Felser, and G. Jakob, Appl. Phys. Lett. **99**, 132509 (2011).